Characterization and Application of Nanomaterials 2026, 9(3), 026260023.
https://doi.org/10.24294/can026260023

Article

Green synthesis of selenium nanoparticles using the aqueous extract of *Catharanthus roseus* (L.) leaves and evaluation of their anticancer activity

Hai Tu Le*, Lan Anh Thi Nguyen, Tuyet Anh Thi Le

Department of Chemistry, The University of Da Nang—University of Science and Education, Da Nang City 550000, Vietnam
*** Corresponding author:** Hai Tu Le, lthai@ued.udn.vn

CITATION

Le H T, Nguyen L A, Le T A. Green synthesis of selenium nanoparticles using the aqueous extract of *Catharanthus roseus* (L.) leaves and evaluation of their anticancer activity. Characterization and Application of Nanomaterials. 2026; 9(3): 026260023. https://doi.org//can026260023

ARTICLE INFO

Received: 07 June 2026
Accepted: 28 July 2026
Available online: 31 August 2026

Abstract: Selenium nanoparticles (SeNPs) have attracted considerable interest for their promising biomedical applications, particularly in cancer therapy. In this study, an environmentally friendly approach was developed to synthesize SeNPs using an aqueous leaf extract of *Catharanthus roseus* (L.), which served as both the reducing and stabilizing agent for converting H_2SeO_3 into elemental selenium nanoparticles. The extraction process was optimized at a leaf-to-water ratio of 20 g per 100 mL of double-distilled water, with boiling for 70 min. The optimal conditions for SeNP synthesis were 12 mL of leaf extract mixed with 30 mL of 5 mM H_2SeO_3 at pH 8 and 80 °C for 105 min. Morphological analysis revealed that the biosynthesized SeNPs were predominantly spherical, with an average particle size of approximately 50 nm. GC–MS and FTIR analyses demonstrated the presence of phytochemicals in the leaf extract that participated in nanoparticle formation while providing surface capping and stabilization. The biological activity of the synthesized SeNPs was evaluated against SK-LU-1, Hep-G2, and MCF-7 cancer cell lines. After 72 h of treatment, the nanoparticles exhibited potent cytotoxicity, with half-maximal inhibitory concentration (IC_{50}) values of 5.54 μg/mL, 4.45 μg/mL, and 4.93 μg/mL, respectively. These findings indicate that *Catharanthus roseus* (L.)-mediated SeNPs represent a simple, sustainable, and effective nanomaterial with promising potential for anticancer applications.

Keywords: green synthesis; *Catharanthus roseus* (L.) leaf; selenium nanoparticles; anticancer; SK-LU1; Hep-G2; MCF7

1. Introduction

Green synthesis has emerged as an environmentally friendly strategy for producing metal nanoparticles by employing plant extracts as both reducing and stabilizing agents. Compared with conventional physical and chemical approaches, such as chemical reduction, thermal reduction, irradiation, and other energy-intensive techniques, plant-mediated synthesis offers a simpler, safer, and more sustainable alternative. During the biosynthesis process, phytochemicals including flavonoids, terpenoids, polyphenols, alkaloids, and reducing sugars donate electrons to metal ions (M^{n+}), converting them into their elemental state (M^0). These reduced atoms subsequently nucleate and grow into nanoparticles, while biomolecules present in the extract adsorb onto the particle surface, preventing aggregation and improving colloidal stability. Owing to its mild reaction conditions, low environmental impact, and elimination of hazardous reducing agents, plant-assisted nanoparticle synthesis has attracted considerable attention as a green alternative to conventional fabrication methods [1–3].

Among various nanomaterials, selenium nanoparticles (SeNPs) have received increasing attention because of their unique physicochemical characteristics and broad

biomedical potential. Green-synthesized SeNPs have demonstrated promising performance in catalysis as well as antibacterial and anticancer applications [4–10]. Several studies have reported that SeNPs exhibit selective cytotoxicity toward cancer cells while causing minimal damage to normal cells. For example, Sonkusre et al. reported the remarkable therapeutic potential of SeNPs against cancer cells [11], whereas Ali et al. demonstrated their inhibitory activity toward lung cancer cells [12]. A wide variety of plant materials have been investigated as reducing agents for SeNP biosynthesis, including lemon leaves [13], raisin leaves and *Catharanthus roseus* flowers [14,15], garlic [16–20], *Aloe vera* leaves [21], broccoli [22], hawthorn fruits [23], Java tea [24], cocoa beans [25], ginger roots [26], hibiscus flowers [27], and neem leaves [28]. These studies collectively demonstrate that plant-derived metabolites can effectively mediate SeNP formation while imparting desirable biological properties to the resulting nanoparticles.

In recent years, many studies by various authors have investigated the synthesis of selenium nanoparticles using plant extracts for biomedical applications such as antimicrobial, antioxidant, antibacterial, cytotoxic, and photocatalytic activities. Vetrivel et al. [29] reported one of the pioneering studies on the green synthesis of SeNPs using *Ceropegia bulbosa* Roxb. tuber extract. The biosynthesized nanoparticles were predominantly spherical and demonstrated multiple biological activities, including antimicrobial, selective cytotoxic, mosquitocidal, and photocatalytic properties. These findings suggest that plant-derived biomolecules not only facilitate the reduction of selenium ions but also form a bioactive surface coating that enhances the functional properties of SeNPs. Ecem and Aydın [30] synthesized SeNPs using *Calluna vulgaris* extract and demonstrated their potent antioxidant activity through DPPH and ABTS radical scavenging assays, together with significant antibacterial effects against both Gram-positive and Gram-negative bacteria. Similarly, Georgia et al. [31] employed *Euphorbia tirucalli* aqueous extract for SeNP biosynthesis and reported promising antimicrobial activity as well as cytotoxic effects against cancer cell lines, highlighting their potential biomedical applications. A comprehensive review by Krystyna [32] emphasized the versatility of plant extracts for producing naturally functionalized SeNPs. The review concluded that the phytochemical composition of each plant extract plays a critical role in determining the reduction efficiency, particle size, morphology, surface charge, and stability of the synthesized nanoparticles. Polyphenols and flavonoids were identified as the primary reducing agents, whereas proteins and polysaccharides mainly contributed to nanoparticle stabilization through surface capping, thereby improving biocompatibility and preventing particle aggregation. In addition to selecting suitable plant sources, recent studies have focused on optimizing synthesis parameters to improve the physicochemical characteristics of SeNPs. Hua et al. [33] synthesized SeNPs using grape seed extract synergistically combined with ascorbic acid to enhance the reduction process. Key synthesis parameters, including pH, temperature, precursor concentration, and extract-to-precursor ratio, were optimized to obtain uniformly distributed nanoparticles with smaller particle sizes and superior antioxidant capacity. The incorporation of ascorbic acid significantly improved both the synthesis efficiency and colloidal stability of the nanoparticles. Beyond biomedical applications, plant-mediated SeNPs have also attracted considerable attention in

sustainable agriculture. Le et al. [34] synthesized SeNPs using *Rosa rugosa* extract and demonstrated their effectiveness against several phytopathogenic microorganisms. The study further elucidated the biosynthesis mechanism, showing that phenolic compounds and flavonoids in the extract were actively involved in selenium reduction. The biosynthesized SeNPs not only exhibited strong antimicrobial activity but also enhanced plant defense responses, suggesting their potential as eco-friendly alternatives to conventional chemical pesticides. Mohamed et al. [35] prepared SeNPs from *Balanites aegyptiaca* extract and comprehensively evaluated their antimicrobial, anticancer, cytogenetic, and molecular docking properties. The nanoparticles exhibited potent inhibitory effects against various pathogenic microorganisms and significantly reduced the viability of cancer cells, primarily through oxidative stress induction and apoptosis-mediated pathways. Likewise, Sama et al. [36] synthesized SeNPs using olive (*Olea europaea*) leaf extract and demonstrated remarkable antimicrobial and antibiofilm activities. The inhibition of biofilm formation is particularly significant because biofilms are closely associated with increased bacterial resistance to antibiotics. The synthesized SeNPs effectively disrupted bacterial cell membranes, induced oxidative stress, and interfered with essential metabolic processes, thereby suppressing both bacterial growth and biofilm development. Halvin and Subramani [37] reported the green synthesis of SeNPs using broccoli (*Brassica oleracea* var. *italica*) extract. The resulting nanoparticles exhibited strong antioxidant and antimicrobial activities against a broad spectrum of pathogenic microorganisms. In addition to experimental validation, molecular docking analysis was performed to elucidate the interactions between SeNP-associated phytochemicals and microbial target proteins, providing mechanistic insights into their antimicrobial effects at the molecular level. Aya et al. [38] synthesized SeNPs using *Aloe vera* leaf extract and investigated their biomedical potential. The biosynthesized nanoparticles exhibited excellent antioxidant, antibacterial, antifungal, anti-inflammatory, wound-healing, and selective anticancer activities while displaying minimal toxicity toward normal cells. These findings indicate that the naturally occurring phytochemicals adsorbed on the nanoparticle surface substantially enhance the biocompatibility and therapeutic potential of plant-mediated SeNPs.

Compared with silver and gold nanoparticles, selenium nanoparticles offer several advantages for biomedical applications. Selenium is an essential trace element involved in antioxidant defense and immune regulation, resulting in lower biological toxicity than many other metallic nanomaterials when administered at appropriate concentrations. Unlike silver nanoparticles, which are primarily valued for their antimicrobial activity but may present toxicity concerns at elevated doses, SeNPs provide both biological functionality and therapeutic potential. In comparison with gold nanoparticles, SeNPs are generally more economical to produce and possess intrinsic biological activity through their participation in selenoprotein-associated antioxidant systems. These characteristics make SeNPs attractive candidates for the development of biocompatible nanomaterials for biomedical applications.

Vietnam possesses abundant medicinal plant resources, many of which contain bioactive phytochemicals suitable for green nanoparticle synthesis. *Catharanthus roseus* (L.), commonly known as Madagascar periwinkle, is a medicinal herb belonging to the Apocynaceae family and is widely cultivated throughout Vietnam

because of its adaptability to tropical climates. Beyond its ornamental value, the plant is recognized as a rich source of pharmacologically active compounds, particularly the alkaloids vincristine and vinblastine, which are widely used in cancer chemotherapy. In addition, its leaves contain flavonoids, terpenoids, carotenoids, and polyphenols that exhibit antioxidant, antibacterial, and antiproliferative activities. These phytochemicals can also function as natural reducing and stabilizing agents during nanoparticle biosynthesis. Consequently, the surface functionalization of SeNPs with these naturally occurring biomolecules may enhance their stability and improve their biomedical performance.

Based on these considerations, the present study aimed to synthesize selenium nanoparticles using an aqueous leaf extract of *Catharanthus roseus* as both the reducing and stabilizing agent. The synthesis conditions were optimized, the physicochemical characteristics of the biosynthesized SeNPs were comprehensively characterized, and their anticancer activities against selected human cancer cell lines were systematically evaluated.

2. Materials and methods

2.1. Materials

Analytical-grade selenious acid (H_2SeO_3), *n*-hexane (C_6H_{14}), chloroform ($CHCl_3$), ethyl acetate ($CH_3COOC_2H_5$), ethanol (C_2H_5OH), sulfuric acid (H_2SO_4), and sodium hydroxide (NaOH) were purchased from Merck (Darmstadt, Germany). Fresh leaves of *Catharanthus roseus* (L.) were collected from Da Nang City, Vietnam. Double-distilled water was used for the preparation of all aqueous solutions throughout the study.

2.2. Preparation of leaf extract

Fresh *Catharanthus roseus* (L.) leaves were thoroughly rinsed with double-distilled water to remove surface impurities and subsequently air-dried at room temperature. The cleaned leaves were then cut into small pieces prior to extraction. To optimize the extraction procedure, the influence of the leaf-to-water ratio and extraction time on the quality of the aqueous extract was systematically evaluated. After boiling under the selected conditions, the resulting extract was filtered through Whatman No. 1 filter paper to remove plant residues. The filtrate was either used immediately for the biosynthesis of selenium nanoparticles or stored at 4 °C until further use.

2.3. Phytochemical screening of aqueous extract of *Catharanthus roseus* (L.) leaf

The aqueous leaf extract of *Catharanthus roseus* (L.) was qualitatively screened for major classes of phytochemicals, including terpenoids, flavonoids, alkaloids, tannins, and saponins, using standard colorimetric assays as previously described [39].

2.4. Chemical constituents of aqueous extract of *Catharanthus roseus* (L.) leaf

The aqueous leaf extract was fractionated by liquid–liquid extraction using *n*-hexane, chloroform, and ethyl acetate to obtain the corresponding solvent fractions. The residual aqueous phase was subsequently concentrated and redissolved in ethanol to prepare the ethanol fraction. All fractions were analyzed using a GC–MS 7890B–5977B system (Agilent Technologies, Santa Clara, CA, USA). Individual constituents were identified by comparing their Kovats retention indices and mass spectral data with those reported by Adams (1989) and the National Institute of Standards and Technology (NIST 98) mass spectral library.

2.5. Synthesis of selenium nanoparticles

Selenium nanoparticles (SeNPs) were synthesized by mixing a predetermined volume of *Catharanthus roseus* (L.) leaf extract with 5 mM H_2SeO_3 solution in a 100 mL Erlenmeyer flask. The reaction mixture was subsequently incubated under the experimental conditions specified for each synthesis experiment.

2.6. Characterization of selenium nanoparticles

The formation of selenium nanoparticles was initially confirmed by UV–Visible spectroscopy. Prior to analysis, the nanoparticle suspension was diluted tenfold with double-distilled water, and the absorption spectra were recorded over the wavelength range of 300–600 nm using a Lambda 365 UV–Visible spectrophotometer (PerkinElmer) at a spectral resolution of 1 nm.

For scanning electron microscopy (SEM), the samples were sputter-coated with gold using a JFC-1600 ion sputter coater (JEOL, Japan) and subsequently examined with a ZEISS EVO MA10 scanning electron microscope (Oberkochen, Germany). Transmission electron microscopy (TEM) analysis was performed by depositing a drop of the SeNP suspension onto carbon-coated copper grids followed by air drying at room temperature. TEM imaging and energy-dispersive X-ray (EDX) analyses were carried out using a Tecnai G2 F20 high-resolution transmission electron microscope (FEI).

The crystalline structure of the synthesized SeNPs was determined by powder X-ray diffraction (XRD) using a PANalytical X'Pert PRO diffractometer. Diffraction patterns were collected over a 2θ range of 10–70°. Fourier transform infrared (FTIR) spectra were recorded using a JASCO FT/IR-6800 spectrometer to identify the functional groups associated with the reduction, surface capping, and stabilization of the biosynthesized SeNPs.

2.7. Evaluation of in vitro cytotoxic activity

The in vitro cytotoxic activity of the synthesized SeNPs was evaluated against three human cancer cell lines, including SK-LU-1 (human lung carcinoma, RRID: CVCL_0629), Hep-G2 (human hepatocellular carcinoma, RRID: CVCL_0027), and MCF-7 (human breast carcinoma, RRID: CVCL_0031). Cytotoxicity assays were performed at the Institute of Biotechnology, Vietnam Academy of Science and Technology, using the sulforhodamine B (SRB) assay.

The as-synthesized SeNP colloidal suspension was serially diluted with culture medium to obtain the desired treatment concentrations. The concentrations are reported as nominal selenium concentrations (μg Se/mL), calculated from the initial amount of H_2SeO_3 used in the optimized synthesis.

Ellipticine was employed as the positive control at concentrations of 10, 2, 0.4, and 0.08 μg/mL, whereas 1% DMSO (final concentration of 0.05% in each well) served as the negative control.

All cytotoxicity experiments were performed in three independent experiments, and the results are expressed as the mean ± standard deviation (SD). IC_{50} values were estimated by nonlinear regression of the dose–response curves using TableCurve 2D v4 software.[40].

3. Results and discussion

3.1. Optimization of *Catharanthus roseus* (L.) leaf extraction

The composition of the *Catharanthus roseus* (L.) leaf extract plays an important role in the biosynthesis of selenium nanoparticles, as it determines the availability of phytochemicals responsible for the reduction and stabilization of SeNPs. Therefore, the extraction process was optimized by evaluating the effects of the leaf-to-water ratio and extraction time on the quality of the obtained extract. To assess the extraction efficiency, each extract was used for SeNP synthesis by reacting 10 mL of the extract with 20 mL of 5 mM H_2SeO_3 in a 100 mL Erlenmeyer flask at 70 °C for 60 min. The characteristic color change of the reaction mixture initially confirmed the formation of SeNPs.

3.1.1. Effect of the leaf-to-water ratio

The influence of the leaf-to-water ratio on SeNP biosynthesis was investigated while maintaining a constant extraction time of 60 min under boiling conditions. The amount of *Catharanthus roseus* (L.) leaves was varied from 5 g to 25 g per 100 mL of double-distilled water (5 g/100 mL, 10 g/100 mL, 15 g/100 mL, 20 g/100 mL, and 25 g/100 mL). The resulting extracts were subsequently employed for SeNP synthesis under identical reaction conditions. As presented in **Figure 1**, the UV–Visible spectra reveal that the leaf-to-water ratio markedly influenced the formation of selenium nanoparticles from the 5 mM H_2SeO_3 precursor solution.

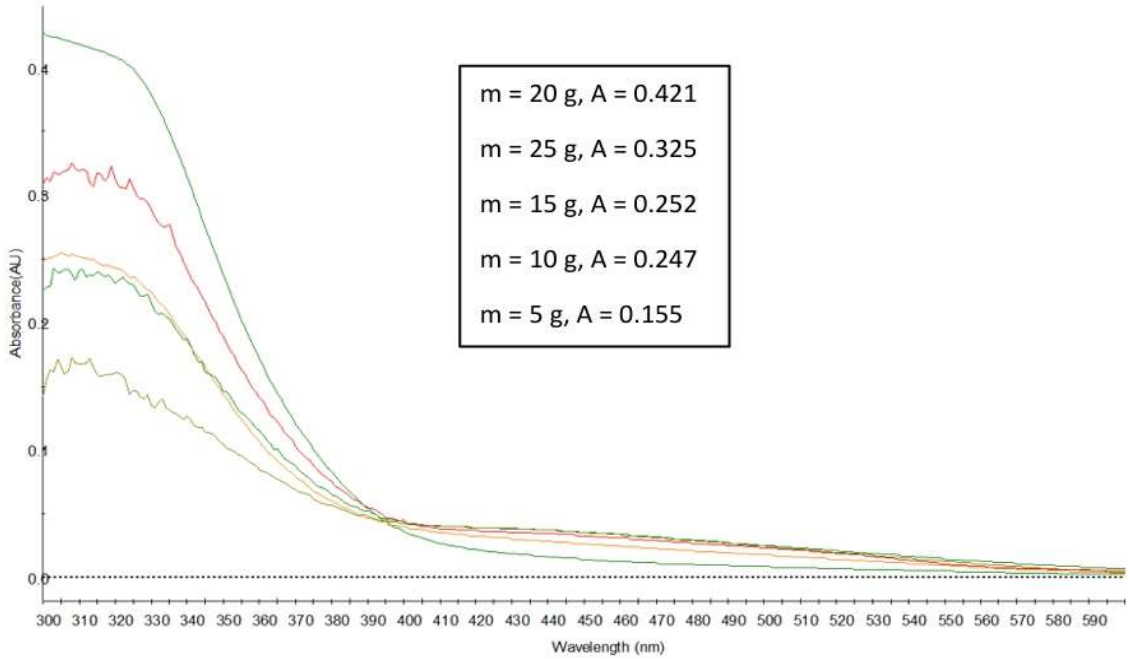

Figure 1. UV–Visible spectra of SeNPs synthesized using *Catharanthus roseus* (L.) leaf extracts prepared at different leaf-to-water ratios. The spectra are arranged from top to bottom based on the mass-dependent influence corresponding to A-values, ordered from highest to lowest to facilitate interpretation. Wavelength range of 300–600 nm and absorbance scale of 0.0–0.4 AU.

Figure 1 illustrates the UV–Visible spectra of SeNPs synthesized using leaf extracts prepared with different leaf-to-water ratios. As the amount of *Catharanthus roseus* (L.) leaves increased from 5 g to 20 g per 100 mL of water, the absorbance intensity gradually increased, indicating enhanced formation of selenium nanoparticles. The highest absorbance was observed at a leaf concentration of 20 g/100 mL, suggesting that this extraction condition provided an adequate amount of phytochemicals capable of reducing H_2SeO_3 and stabilizing the resulting nanoparticles.

When the leaf content was further increased to 25 g/100 mL, the absorbance intensity decreased. A possible explanation is that the higher concentration of plant-derived compounds accelerated the reduction process, promoting rapid nucleation followed by particle growth and partial aggregation. The formation of larger nanoparticles or aggregates may reduce the characteristic absorbance intensity of the colloidal suspension. Similar behavior has been reported in plant-mediated nanoparticle synthesis, where excessive concentrations of reducing biomolecules can alter nanoparticle growth kinetics and colloidal stability. Therefore, a leaf-to-water ratio of 20 g per 100 mL was selected as the optimum condition for subsequent experiments.

3.1.2. Effect of extraction time

The influence of extraction time on the biosynthesis of selenium nanoparticles was investigated using *Catharanthus roseus* (L.) leaf extract prepared with a leaf-to-water ratio of 20 g/100 mL under boiling conditions. The extraction time was varied from 50 min to 90 min (50 min, 60 min, 70 min, 80 min, and 90 min), while all other extraction parameters were kept constant. The resulting extracts were subsequently

used for SeNP synthesis under identical reaction conditions. The corresponding UV–Visible spectra are presented in **Figure 2**.

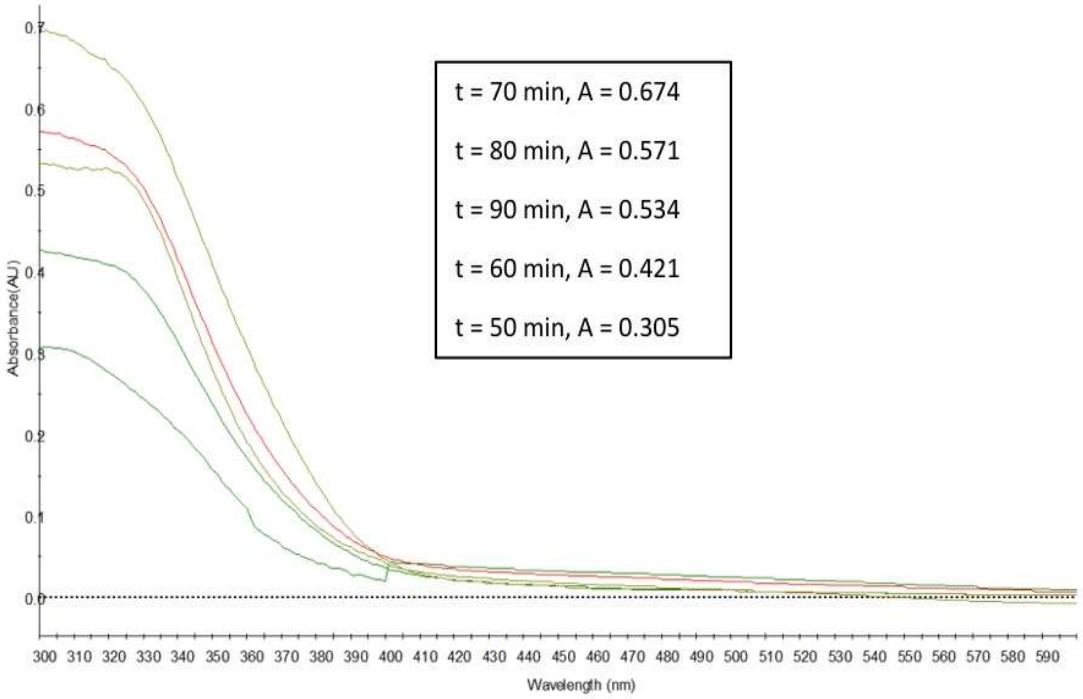

Figure 2. UV–Visible spectra of SeNPs synthesized using *Catharanthus roseus* (L.) leaf extracts prepared at different extraction times. The spectra are arranged from top to bottom based on the extraction time-dependent influence corresponding to A-values, ordered from highest to lowest to facilitate interpretation. Wavelength range of 300–600 nm and absorbance scale of 0.0–0.7 AU.

As shown in **Figure 2**, the absorbance intensity of the synthesized SeNPs gradually increased as the extraction time was extended from 50 min to 70 min, reaching a maximum at 70 min. This result suggests that prolonging the extraction process enhanced the release of phytochemicals, including flavonoids, polyphenols, and other reducing compounds, thereby improving the reduction of H_2SeO_3 and promoting SeNP formation.

When the extraction time was further increased beyond 70 min, the absorbance intensity decreased. A possible explanation is that prolonged heating may lead to the degradation or oxidation of certain bioactive compounds, reducing their reducing capacity. In addition, excessive extraction of plant constituents may alter the nucleation and growth processes of SeNPs, resulting in particle aggregation and a corresponding decrease in absorbance intensity. Similar observations have been reported in plant-mediated nanoparticle synthesis, where excessive extraction can adversely affect nanoparticle formation and colloidal stability. Therefore, an extraction time of 70 min was selected as the optimum condition for preparing *Catharanthus roseus* leaf extract.

Based on the optimization results, the optimum extraction conditions consisted of a leaf-to-water ratio of 20 g/100 mL, an extraction time of 70 min, and extraction under boiling conditions. These parameters were adopted for all subsequent experiments.

3.2. Phytochemical screening of the aqueous leaf extract of *Catharanthus roseus* (L.)

Qualitative phytochemical screening was performed to identify the major classes of bioactive metabolites present in the aqueous leaf extract of *Catharanthus roseus* (L.). The extract was examined for the presence of flavonoids, terpenoids, alkaloids, saponins, and tannins using standard phytochemical assays. The results of the qualitative screening are summarized in **Table 1**.

As shown in Table 1, the aqueous leaf extract of *Catharanthus roseus* (L.) tested positive for flavonoids, terpenoids, alkaloids, saponins, and tannins. The presence of these phytochemicals indicates that the extract contains a diverse range of bioactive compounds capable of participating in the green synthesis of selenium nanoparticles. These metabolites can act as natural reducing agents by converting Se(IV) ions into elemental selenium, while simultaneously serving as capping and stabilizing agents that enhance the stability of the synthesized SeNPs.

Table 1. Phytochemical screening of aqueous extract of *Catharanthus roseus* (L.) leaf.

Phytochemical	***Catharanthus roseus* (L.) leaf extract**
Flavonoids	+
Terpenoids	+
Alkaloids	+
Saponin	+
Tannin	+

Note: + indicates present.

3.3. Chemical constituents of *Catharanthus roseus* (L.) leaf aqueous extract identified by GC–MS

The chemical composition of the aqueous leaf extract of *Catharanthus roseus* (L.) was analyzed by GC–MS, and the identified constituents are summarized in **Table 2**.

As shown in **Table 2**, the aqueous extract contained several phytosterols, including campesterol, stigmasterol, and γ-sitosterol. The presence of these phytosterols, together with other phytochemicals identified in the qualitative screening, suggests that the extract is a rich source of bioactive compounds involved in nanoparticle biosynthesis. These metabolites may contribute to the reduction of selenium ions and subsequently adsorb onto the nanoparticle surface, acting as capping and stabilizing agents that improve the stability of the synthesized SeNPs. Similar roles of plant-derived phytochemicals in the green synthesis of metal nanoparticles have been reported previously [41].

Table 2. GC-MS analysis of *Catharanthus roseus* (L.) leaf aqueous extract.

Compound	Chemical formula
1-Hydroxy-3-methyl-9H-carbazol	$C_{13}H_{11}NO$
n-Hexadecanoic acid	$C_{16}H_{32}O_2$
Phytol	$C_{20}H_{40}O$
Isovindolinine	C_8H_7NO
Vindolinine	$C_{25}H_{32}N_2O_6$
Squalene	$C_{30}H_{50}$
4-((1E)-3-Hydroxy-1-propenyl)-2-methoxyphenol	$C_{10}H_{12}O_3$
Campesterol	$C_{28}H_{48}O$
Stigmasterol	$C_{29}H_{48}O$
γ-Sitosterol	$C_{29}H_{50}O$
Vitamin E	

3.4. Effect of factors on the synthesis of selenium nanoparticles

The effects of several experimental parameters, including the volume ratio of *Catharanthus roseus* (L.) leaf extract to H_2SeO_3 solution, reaction temperature, pH, and reaction time, on the biosynthesis of selenium nanoparticles (SeNPs) were systematically investigated. These parameters were optimized to identify the conditions that favor efficient nanoparticle formation and improve the quality of the synthesized SeNPs.

3.4.1. Effect of the volume ratio of *Catharanthus roseus* (L.) leaf extract

The influence of the volume ratio between the *Catharanthus roseus* (L.) leaf extract and H_2SeO_3 solution on the biosynthesis of selenium nanoparticles was investigated under fixed reaction conditions. The synthesis was carried out using 30 mL of 5 mM H_2SeO_3 solution at 70 °C for 60 min, while the volume of leaf extract was varied from 6 mL to 14 mL. All other reaction parameters were kept constant throughout the experiments. The UV–Visible spectra of the synthesized SeNPs obtained under different extract volumes are presented in **Figure 3.**

As shown in **Figure 3**, increasing the volume of *Catharanthus roseus* (L.) leaf extract from 6 mL to 12 mL resulted in a gradual increase in the absorbance intensity of the characteristic SeNP band. The highest absorbance was obtained at an extract volume of 12 mL, suggesting that this condition provided a sufficient amount of phytochemicals to reduce H_2SeO_3 and promote the formation of selenium nanoparticles efficiently.

Further increasing the extract volume beyond 12 mL led to a decrease in absorbance intensity. A possible explanation is that an excessive concentration of plant-derived biomolecules accelerated the reduction process, resulting in rapid nucleation followed by particle growth and partial aggregation. The formation of larger particles or aggregates may reduce the characteristic absorbance of the colloidal SeNP suspension. Similar effects have been reported in green nanoparticle synthesis when an excess of reducing and capping agents alters nanoparticle growth kinetics

[41]. Therefore, an extract volume of 12 mL per 30 mL of 5 mM H_2SeO_3 solution was selected as the optimum condition for subsequent experiments.

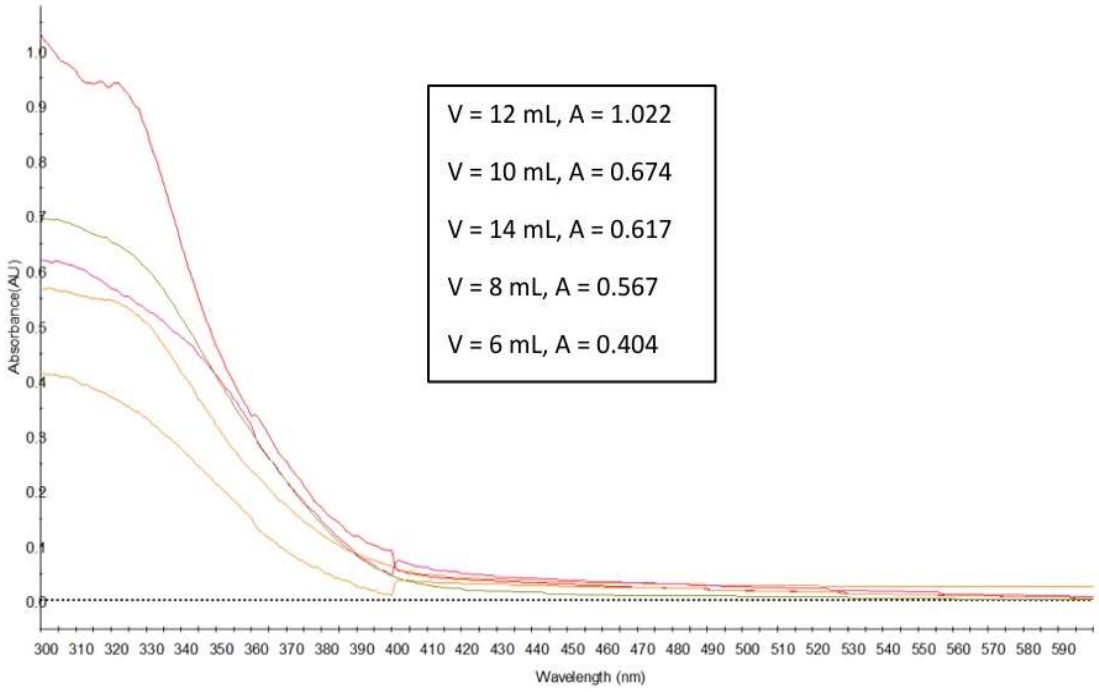

Figure 3. UV–Visible spectra of SeNPs synthesized using different volumes of *Catharanthus roseus* (L.) leaf extract with 30 mL of 5 mM H_2SeO_3 solution. The spectra are arranged from top to bottom based on the extraction time-dependent influence corresponding to A-values, ordered from highest to lowest to facilitate interpretation. Wavelength range of 300–600 nm and absorbance scale of 0.0–1.0 AU.

3.4.2. Effect of temperature on the biosynthesis of selenium nanoparticles

Temperature is one of the key parameters influencing the biosynthesis of metal nanoparticles because it affects both the reduction kinetics of metal ions and the growth of nanoparticles. In this study, the effect of reaction temperature on SeNP formation was investigated under fixed reaction conditions, including a synthesis time of 60 min and a leaf extract-to-H_2SeO_3 volume ratio of 12 mL:30 mL. The reaction temperature was varied from 60 °C to 100 °C (60 °C, 70 °C, 80 °C, 90 °C, and 100 °C), while all other experimental parameters were maintained constant. The corresponding UV–Visible spectra of the synthesized SeNPs are presented in **Figure 4**.

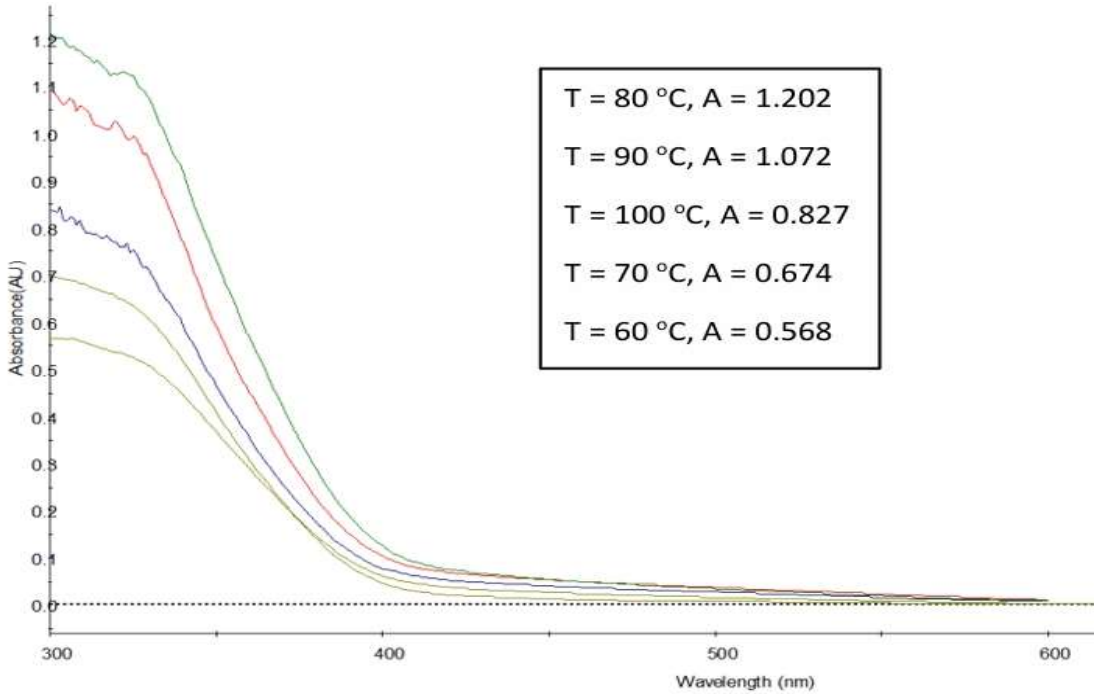

Figure 4. UV–Visible spectra of SeNPs synthesized at different reaction temperatures. The spectra are arranged from top to bottom based on the reaction temperatures -dependent influence corresponding to A-values, ordered from highest to lowest to facilitate interpretation. Wavelength range of 300–600 nm and absorbance scale of 0.0–1.2 AU.

As shown in **Figure 4**, the absorbance intensity of the synthesized SeNPs increased with increasing reaction temperature and reached a maximum at 80 °C. This result indicates that elevating the reaction temperature accelerated the reduction of H_2SeO_3 by the phytochemicals present in the *Catharanthus roseus* (L.) leaf extract, thereby promoting the formation of selenium nanoparticles. However, a further increase in temperature resulted in a decrease in absorbance intensity. A possible explanation is that excessive heating enhanced particle growth and aggregation, leading to the formation of larger SeNPs with reduced colloidal stability and, consequently, lower absorbance. Therefore, 80 °C was selected as the optimum reaction temperature for the biosynthesis of SeNPs.

3.4.3. Effect of pH on the biosynthesis of SeNPs

The pH of the plant extract is an important factor influencing the green synthesis of selenium nanoparticles because it affects both the ionization state of phytochemicals and the reduction kinetics of selenium ions [42]. The influence of pH on SeNP biosynthesis was investigated by adjusting the pH of the *Catharanthus roseus* (L.) leaf extract while maintaining all other reaction conditions constant. The resulting UV–Visible spectra of the synthesized SeNPs are presented in **Figure 5**.

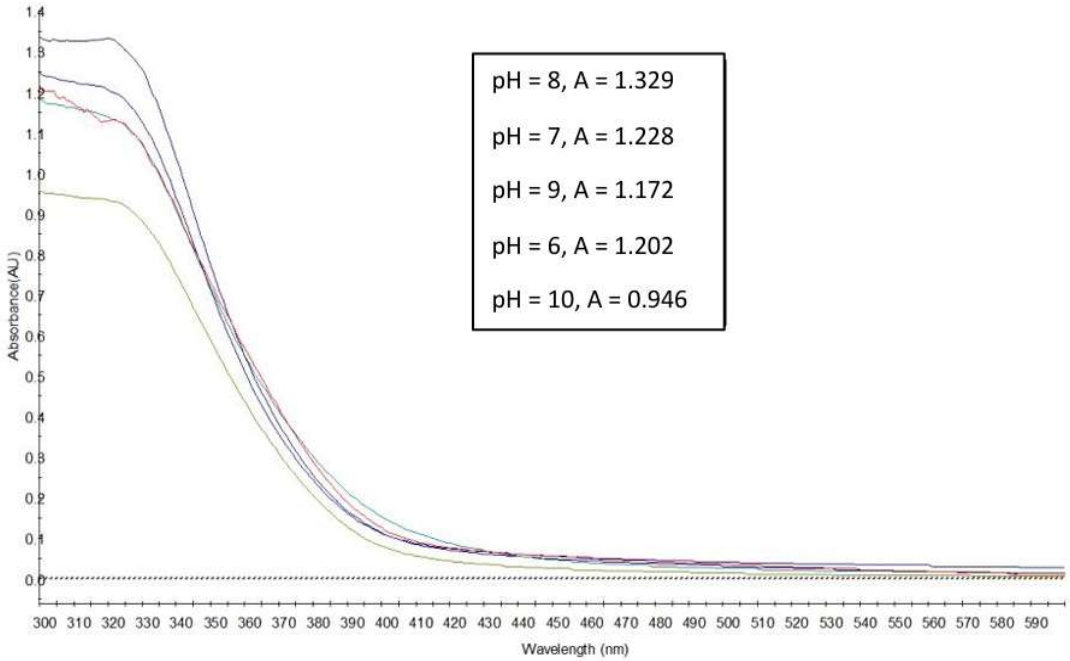

Figure 5. UV–Visible spectra of SeNPs synthesized at different pH values. The spectra are arranged from top to bottom based on the reaction temperatures -dependent influence corresponding to A-values, ordered from highest to lowest to facilitate interpretation. Wavelength range of 300–600 nm and absorbance scale of 0.0–1.4 AU.

As shown in **Figure 5**, the absorbance intensity of the synthesized SeNPs increased as the pH was raised from 6 to 8, reaching a maximum at pH 8. This observation suggests that mildly alkaline conditions enhanced the reducing ability of the phytochemicals present in the *Catharanthus roseus* (L.) leaf extract, thereby promoting the formation of selenium nanoparticles. At higher pH values (9 and 10), the absorbance intensity decreased. A possible explanation is that the elevated alkalinity accelerated the reduction of selenium ions, resulting in rapid nucleation followed by particle growth and partial aggregation. The formation of larger nanoparticles or aggregates reduced the colloidal stability of the suspension and consequently decreased the absorbance intensity. Therefore, pH 8 was selected as the optimum pH for SeNPs biosynthesis.

3.4.4. Effect of reaction time on the biosynthesis of selenium nanoparticles

Reaction time is another important parameter affecting the biosynthesis of selenium nanoparticles, as it influences both the reduction of selenium ions and the growth of nanoparticles. The effect of reaction time on SeNP formation was investigated by varying the reaction duration while maintaining all other experimental conditions constant. The resulting UV–Visible spectra of the synthesized SeNPs are presented in **Figure 6**.

As shown in **Figure 6**, the UV–Vis spectra exhibited a characteristic absorption band in the range of 320–330 nm throughout the reaction. As the reaction time increased, the absorbance intensity gradually increased, indicating the progressive reduction of Se(IV) ions by phytochemicals in the *Catharanthus roseus* (L.) leaf extract and the formation of SeNPs. Notably, the position of the absorption maximum

remained essentially unchanged, suggesting that the nanoparticles formed with relatively consistent optical characteristics during the synthesis process. No further significant increase in absorbance was observed after 105 min, indicating that the reaction had reached a stable stage under the experimental conditions.

Based on the optimization results, the optimum conditions for the biosynthesis of SeNPs were an extract-to-H_2SeO_3 volume ratio of 12 mL:30 mL (5 mM H_2SeO_3), pH 8, a reaction temperature of 80 °C, and a reaction time of 105 min. These conditions were used in all subsequent experiments.

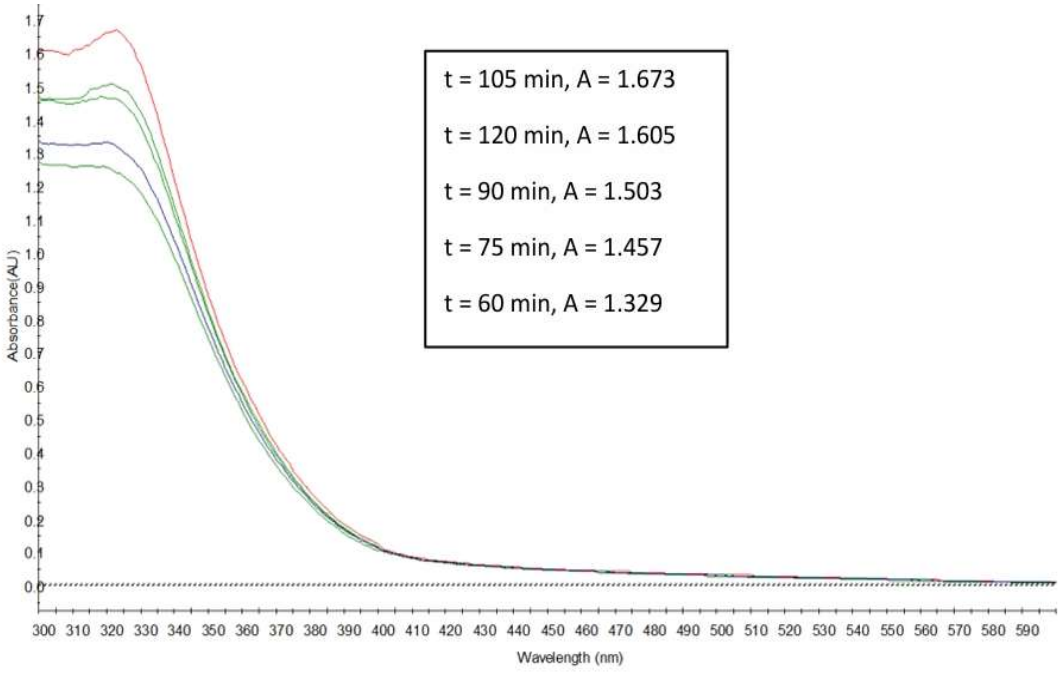

Figure 6. UV–Visible spectra of SeNPs synthesized at different reaction times. The spectra are arranged from top to bottom based on the reaction temperatures -dependent influence corresponding to A-values, ordered from highest to lowest to facilitate interpretation. Wavelength range of 300–600 nm and absorbance scale of 0.0–1.7 AU.

3.5. FE-SEM, TEM, DLS, Zeta potential, EDX, and XRD characterization of selenium nanoparticles

The morphology and microstructure of the biosynthesized SeNPs were examined by FE-SEM and TEM, and the corresponding images are presented in **Figure 7**. Both FE-SEM and TEM observations revealed that the synthesized nanoparticles were predominantly spherical and well dispersed, with an average particle diameter of approximately 50 nm. The relatively uniform particle morphology indicates that the phytochemicals present in the *Catharanthus roseus* (L.) leaf extract effectively regulated nanoparticle growth and contributed to the stabilization of the colloidal SeNPs.

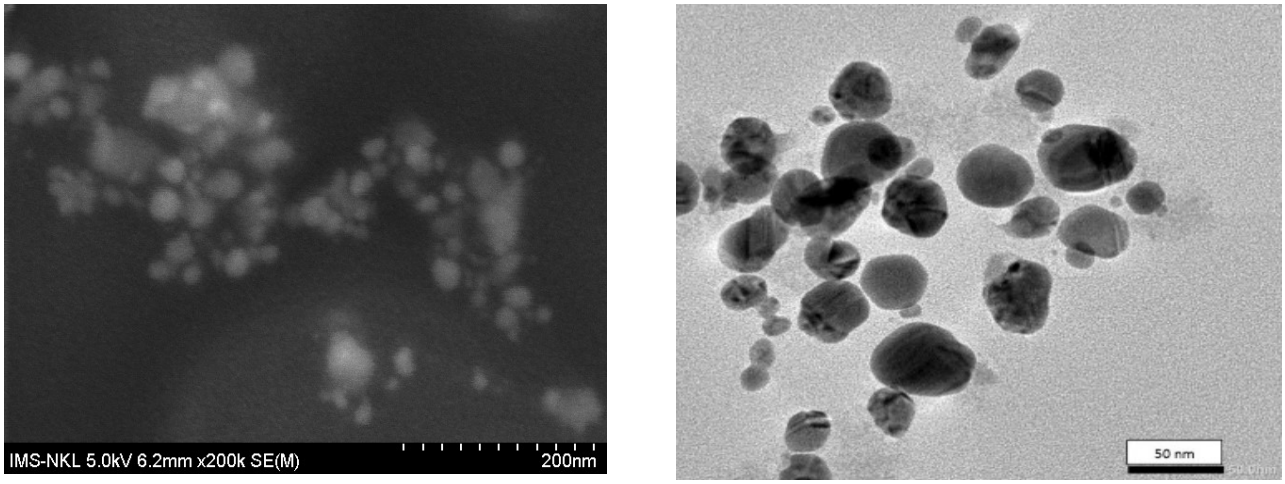

Figure 7. FE-SEM and TEM micrographs of SeNPs biosynthesized using the aqueous leaf extract of *Catharanthus roseus* (L.).

Dynamic light scattering (DLS) analysis (**Figure 8**) was performed to evaluate the hydrodynamic particle size distribution of the biosynthesized SeNPs dispersed in an aqueous medium. The nanoparticles exhibited D10, D50, and D90 values of 28.8, 35.2, and 49.5 nm, respectively, indicating a relatively narrow size distribution. The polydispersity index (PDI) was 0.277, further confirming the moderate uniformity of the synthesized nanoparticles.

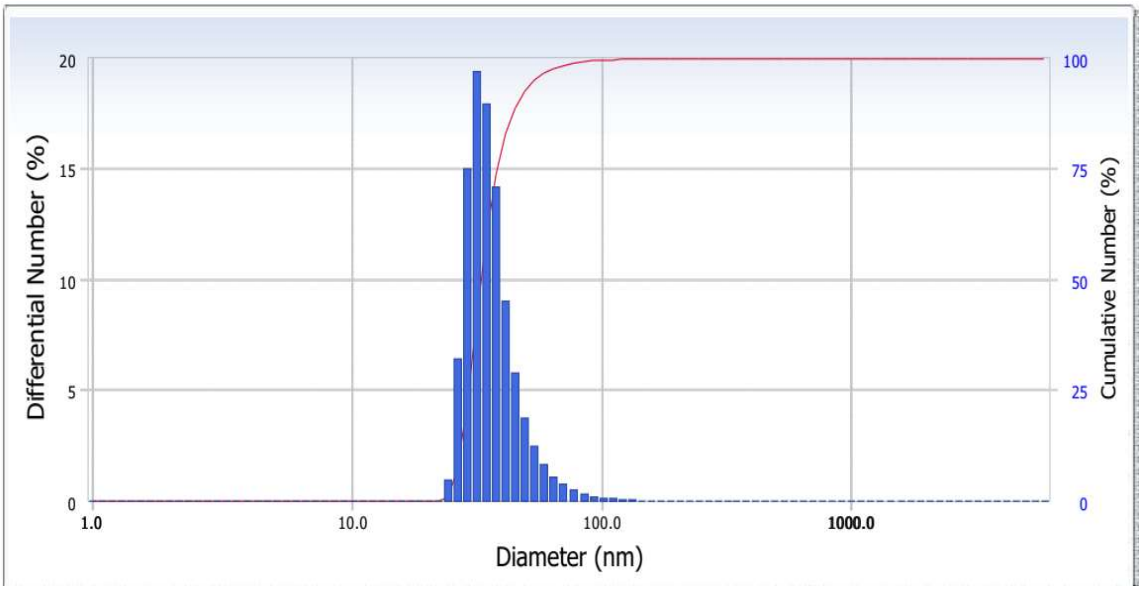

Figure 8. Size distribution mean of biosynthesized SeNPs from *Catharanthus roseus* (L.) leaf extracts in nm.

The measured zeta potential of −15.4 mV (**Figure 9**) suggests that the biosynthesized SeNPs possess moderate colloidal stability. Although nanoparticles with absolute zeta potential values exceeding ±30 mV are generally considered highly stable due to strong electrostatic repulsion, the stability of plant-mediated SeNPs is also influenced by steric stabilization provided by phytochemicals adsorbed on the nanoparticle surface. The relatively low PDI value (0.277) further indicates a

reasonably uniform particle size distribution, supporting the formation of a moderately stable colloidal suspension.

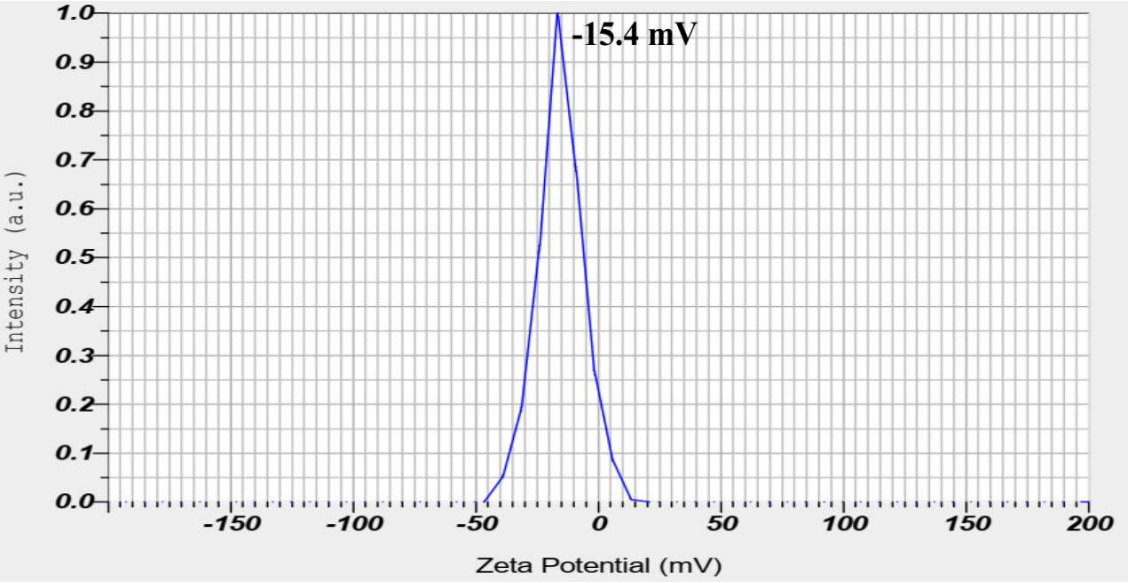

Figure 9. Zeta potential of SeNPs from *Catharanthus roseus* (L.) leaf extracts in mV.

The EDX spectrum (**Figure 10**) confirms the presence of selenium as the major elemental constituent of the synthesized nanoparticles. Signals corresponding to carbon and oxygen were also detected, which can be attributed to phytochemicals adsorbed on the nanoparticle surface and the supporting carbon film used for TEM/EDX measurements. These results support the successful formation of selenium nanoparticles and indicate that selenium is the predominant elemental component of the synthesized sample.

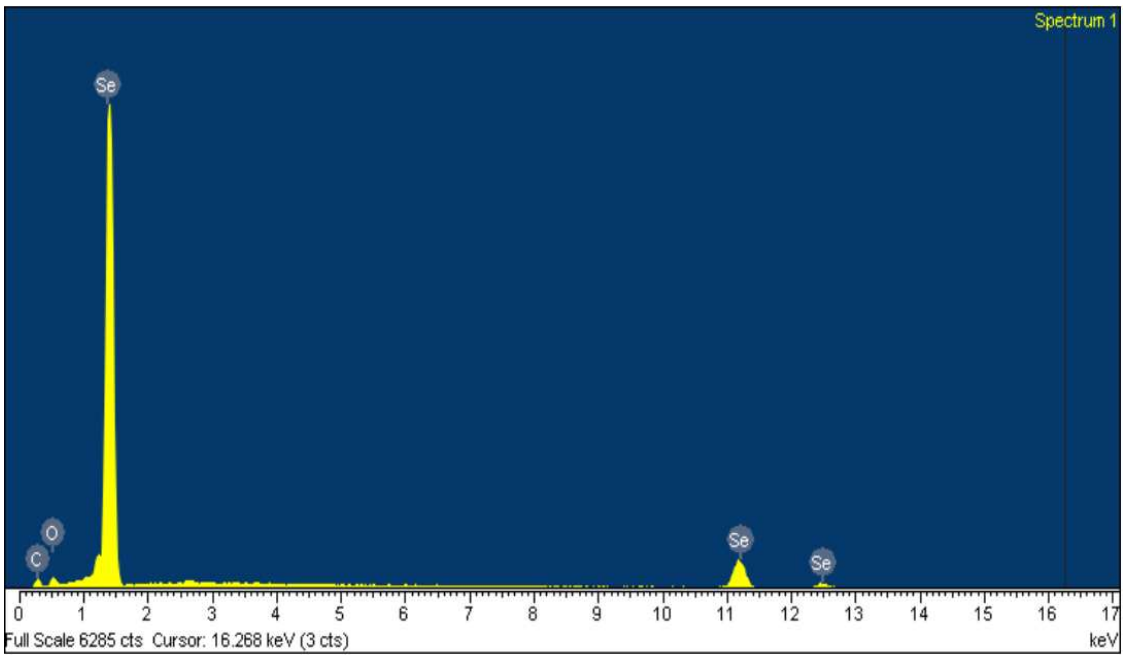

Figure 10. EDX spectrum of SeNPs biosynthesized using the aqueous leaf extract of *Catharanthus roseus* (L.).

The X-ray diffraction (XRD) pattern of SeNPs biosynthesized using the aqueous leaf extract of *Catharanthus roseus* (L.) is presented in **Figure 11**.

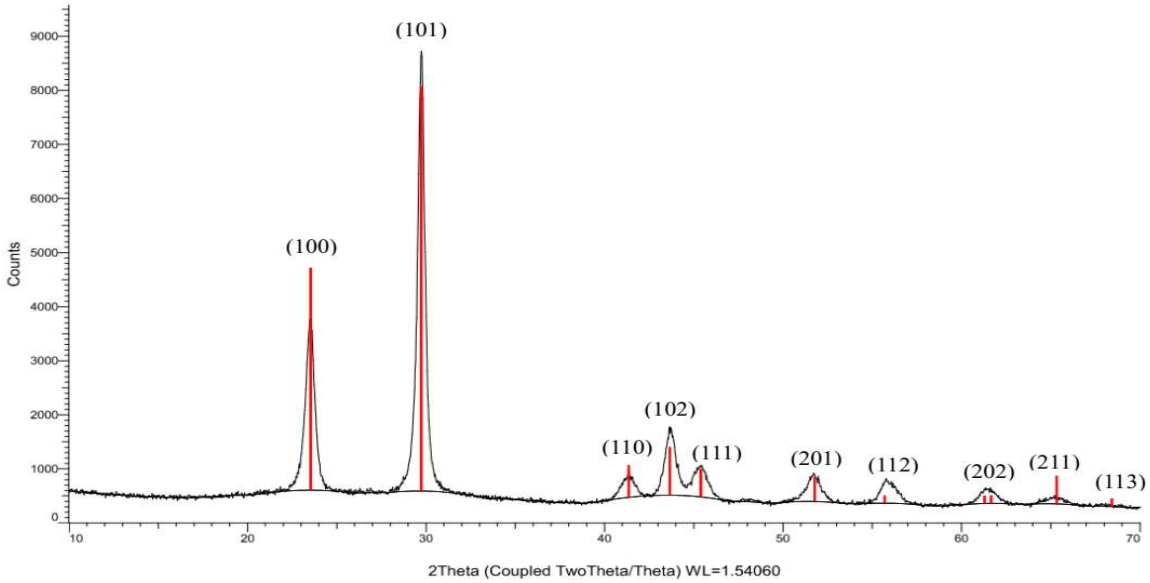

Figure 11. XRD pattern of SeNPs biosynthesized using the aqueous leaf extract of *Catharanthus roseus* (L.).

The diffraction peaks observed at 2θ = 23.7°, 29.8°, 41.4°, 43.9°, 45.5°, 51.8°, 56.3°, 61.9°, 65.2°, and 68.6° were indexed to the (100), (101), (110), (102), (111), (201), (112), (202), (211), and (113) crystal planes, respectively, confirming the crystalline nature of the synthesized SeNPs.

3.6. FTIR analysis of *Catharanthus roseus* (L.) leaf extract and biosynthesized SeNPs

Fourier-transform infrared (FTIR) spectroscopy was employed to identify the functional groups and bioactive compounds involved in the reduction and stabilization of selenium nanoparticles. Particular attention was given to the phytochemicals that may act as reducing, capping, and stabilizing agents during the biosynthesis process. The FTIR spectra of the aqueous leaf extract of *Catharanthus roseus* (L.) (spectrum A) and the biosynthesized SeNPs (spectrum B) are presented in **Figure 12**.

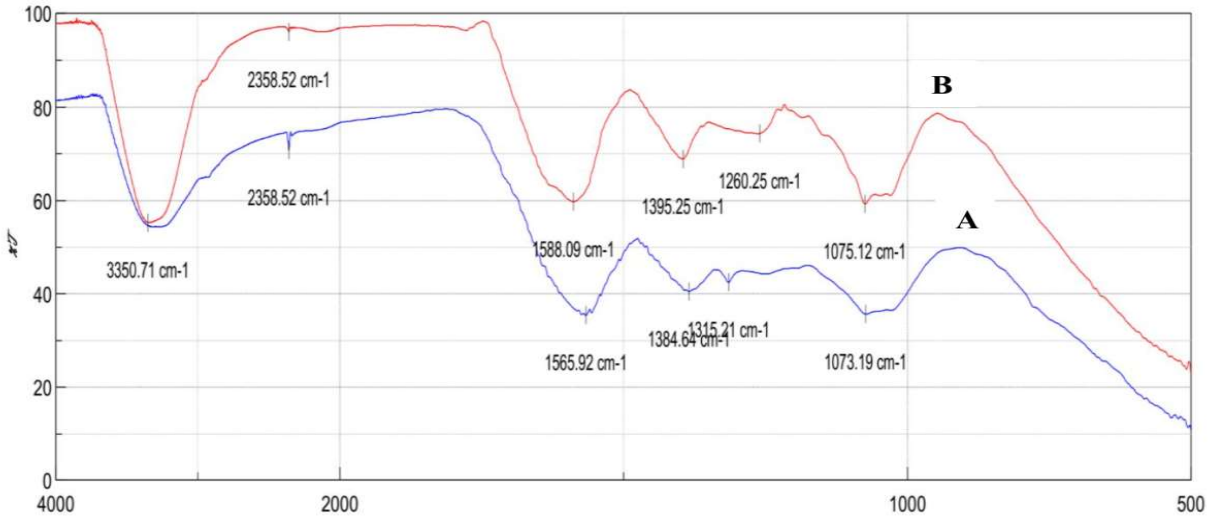

Figure 12. FTIR spectra of the aqueous leaf extract of *Catharanthus roseus* (L.) (A) and biosynthesized SeNPs (B).

The FTIR spectra of the aqueous leaf extract and the biosynthesized SeNPs are presented in **Figure 12A** and **Figure 12B**, respectively. The leaf extract exhibited characteristic absorption bands at 3350.71, 2358.52, 1565.92, 1384.64, 1315.21, and 1073.19 cm^{-1}, whereas the corresponding bands of the SeNPs appeared at 3350.71, 2358.52, 1588.09, 1395.25, 1260.25, and 1075.12 cm^{-1}.

The broad absorption band centered at approximately 3351 cm^{-1} is attributed to the stretching vibration of hydroxyl (–OH) groups, indicating the presence of alcohols and phenolic compounds in the plant extract. The absorption band near 2359 cm^{-1} was observed in both spectra and may be associated with atmospheric CO_2 or weak stretching vibrations of organic functional groups. The bands located at 1565–1588 cm^{-1} are assigned to carbonyl- or aromatic-related functional groups, whereas the absorption bands in the 1260–1395 cm^{-1} region are associated with C–O–C and C–O stretching vibrations of oxygen-containing phytochemicals. The absorption band around 1074 cm^{-1} is attributed to C–O stretching vibrations of ester or alcohol groups.

Compared with the spectrum of the leaf extract, slight shifts in several absorption bands were observed after nanoparticle synthesis. These spectral changes indicate that the corresponding functional groups participated in the reduction of H_2SeO_3 and subsequently remained adsorbed on the nanoparticle surface as capping and stabilizing agents. The preservation of the major absorption bands in the SeNP spectrum further suggests that phytochemicals derived from the *Catharanthus roseus* (L.) leaf extract contributed to the stabilization of the biosynthesized SeNPs and helped prevent nanoparticle aggregation.

3.7. The mechanism of the formation of selenium nanoparticles by aqueous extract of *Catharanthus roseus* (L.) leaf

Based on the results of phytochemical screening and determination of chemical compositions by GC-MS, the aqueous extract of *Catharanthus roseus* (L.) leaf contains campesterol, stigmasterol, γ-sitosterol; these substances contain hydroxyl groups will act as the reducing agent H_2SeO_3 to Se [32].

The oxidation reactions of the phytochemicals can be represented as follows:

$$\text{Campesterol} \rightarrow \text{Campestenone} + 2H^+ + 2e$$

$$\text{Stigmasterol} \rightarrow \text{Stigmasterone} + 2H^+ + 2e$$

$$\gamma\text{-Sitosterol} \rightarrow \gamma\text{-Sitostenone} + 2H^+ + 2e$$

The reduction of selenous acid (H_2SeO_3) to elemental selenium (Se^0) can be represented by the following reaction:

$$H_2SeO_3 + 4e + 4H^+ \rightarrow Se + 3H_2O$$

The biosynthesized SeNPs are likely stabilized through interactions between their surface and the oxygen-containing functional groups of phytochemicals present in the *Catharanthus roseus* (L.) leaf extract. In particular, the lone-pair electrons of oxygen atoms and the π electrons of the carbonyl (C=O) groups in compounds such as campestenone, stigmasterone, γ-sitostenone, together with other phytochemicals, may coordinate with the nanoparticle surface, thereby acting as capping and stabilizing agents.

3.8. Anticancer activity of selenium nanoparticles

The in vitro cytotoxic activity of the biosynthesized SeNPs was evaluated against three human cancer cell lines, namely SK-LU-1 (human lung carcinoma), Hep-G2 (human hepatocellular carcinoma), and MCF-7 (human breast carcinoma). Cell viability was assessed after 72 h of treatment using the sulforhodamine B (SRB) colorimetric assay.

Representative microscopic images showing the effects of SeNP treatment on the tested cancer cell lines are presented in **Figure 13**, while the corresponding cytotoxicity results are summarized in **Table 3**.

As shown in **Table 3**, the biosynthesized SeNPs exhibited significant cytotoxic activity against all three tested cancer cell lines. The IC_{50} values were 5.54 µg/mL for SK-LU-1, 4.45 µg/mL for Hep-G2, and 4.93 µg/mL for MCF-7 cells. Among the tested cell lines, Hep-G2 and MCF-7 cells showed slightly greater sensitivity to SeNP treatment than SK-LU-1 cells.

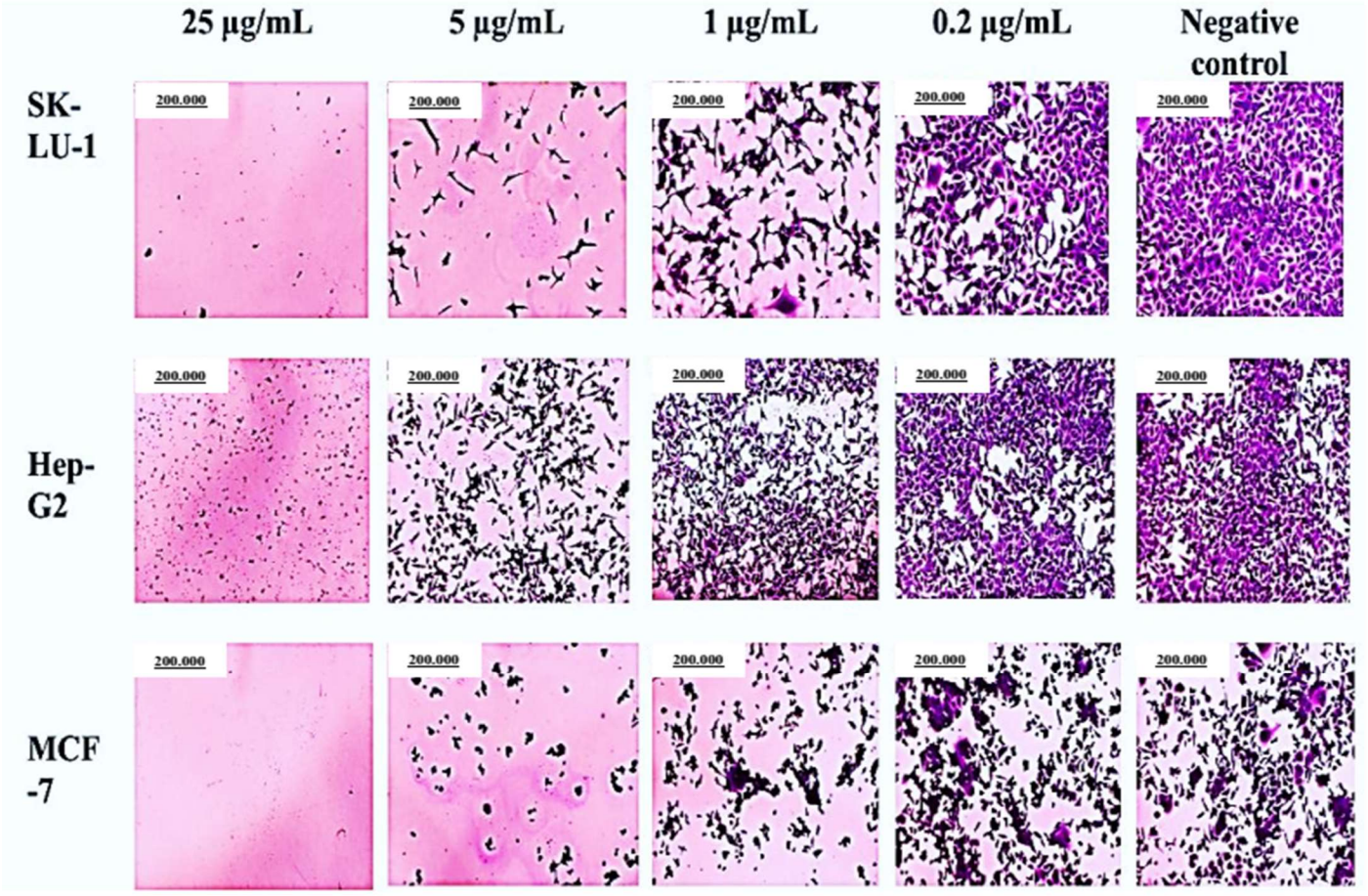

Figure 13. Anticancer activity of *Catharanthus roseus* (L.) leaf selenium nanoparticles against SK-LU-1, Hep-G2, and MCF-7 cell lines.

Table 3. In vitro cytotoxicity effect of selenium nanoparticles from *Catharanthus roseus* (L.) leaf on cancer cell lines, represented as cell inhibition percentage ± standard deviation.

Concentration (µg/mL)	SK-LU-1		Hep-G2		MCF-7	
	% of inhibition	SD	% of inhibition	SD	% of inhibition	SD
25	99.83	2.26	98.42	0.86	98.73	1.28
5	45.48	1.97	55.08	1.20	52.52	1.41
1	27.03	0.96	21.42	1.78	20.80	0.35
0.2	9.71	0.84	10.62	0.85	11.89	1.31
IC50	5.54 ± 0.47		4.45 ± 0.32		4.93 ± 0.39	

SD = Standard deviation.

The IC_{50} values obtained for MCF-7 cells (4.93 µg/mL) and Hep-G2 (4.45 µg/mL) are lower than those reported for SeNPs synthesized using several other plant extracts [38,43,44]. It is evident that the IC_{50} values of synthesized SeNPs by *Catharanthus roseus* (L.) leaf extract were significantly lower than that of the reported SeNPs. This enhanced activity may be associated with phytosterols, including campesterol, stigmasterol, and γ-sitosterol, identified in the *Catharanthus roseus* (L.) leaf extract, which have been reported to exhibit anticancer properties [45–47]. These phytochemicals may remain associated with the green-synthesized SeNP colloidal

system and contribute synergistically to the observed cytotoxic activity. However, since the cytotoxic activity of the *Catharanthus roseus* (L.) leaf extract alone was not evaluated, the relative contributions of the phytochemicals and the selenium nanoparticles cannot be distinguished in the present study.

Overall, the results demonstrate that the SeNPs synthesized using the aqueous leaf extract of *Catharanthus roseus* (L.) exhibit promising in vitro cytotoxic activity against SK-LU-1, Hep-G2, and MCF-7 human cancer cell lines, supporting their potential for further investigation as anticancer nanomaterials.

4. Conclusions

Selenium nanoparticles (SeNPs) were successfully biosynthesized using the aqueous leaf extract of *Catharanthus roseus* (L.) as both the reducing and stabilizing agent. The optimum synthesis conditions were an extract-to-H_2SeO_3 volume ratio of 12 mL:30 mL (5 mM H_2SeO_3), pH 8, a reaction temperature of 80 °C, and a reaction time of 105 min, using leaf extract prepared from 20 g of leaves per 100 mL of water with an extraction time of 70 min.

The biosynthesized SeNPs were predominantly spherical with an average particle size of approximately 50 nm. FTIR analysis indicated that phytochemicals present in the leaf extract participated in the reduction of H_2SeO_3 and subsequently acted as capping and stabilizing agents, while XRD and EDX analyses confirmed the successful formation and elemental composition of the SeNPs.

The synthesized SeNPs exhibited significant in vitro cytotoxic activity against SK-LU-1, Hep-G2, and MCF-7 human cancer cell lines, with IC_{50} values of 5.54, 4.45, and 4.93 μg/mL, respectively. These findings suggest that *Catharanthus roseus* (L.) leaf extract is a promising natural resource for the green synthesis of biologically active SeNPs and that the resulting nanoparticles warrant further investigation for potential biomedical applications, particularly in cancer therapy.

Author contributions: Conceptualization, HTL; formal analysis, HTL, LATN, TATL; investigation, HTL, LATN, TATL; methodology, HTL; visualization, LATN; writing – original draft, HTL; writing – review and editing, HTL, LATN. All authors have read and agreed to the published version of the manuscript.

Ethics approval and consent to participate: Ethical Statements: The SK-LU-1, Hep-G2, and MCF-7 cell lines were provided by Prof. Chi Ying F Huang, National Yang Ming Chiao Tung University, Taipei, Taiwan. Ethic Issue: This study involved only established human cancer cell lines for in vitro experiments and did not involve human participants, human tissues, clinical samples, or experimental animals. Therefore, institutional ethical approval was not required.

Conflict of interest: The authors declare no conflicts of interest.

References

1. Mumtaz A, Mohammad A, Ahmad S. Role of natural products in green synthesis of nanoparticles. In: Green Biosynthesis of Nanoparticles Mechanisms and Applications. Printed and Bound in the UK by Berforts Information Press Ltd. 2013; 31-52.
2. Mittal K, Chisti Y, Banerjee C. Synthesis of metallic nanoparticles using plants. Biotechnology Advances. 2013; 31, 346-356.

3. Salem S, Fouda A. Green Synthesis of Metallic Nanoparticles and Their Prospective Biotechnological Applications: An Overview. Biological Trace Element Research. 2020.
4. Karthik K, Binoy C, Rajeshkumar S, et al. A review on selenium nanoparticles and their biomedical applications. Biomedical Technology. 2024; 6, 61-74.
5. Ramya S, Shanmugasundaram T, Balagurunathan R. Biomedical potential of actinobacterially synthesized selenium nanoparticles with special reference to anti-biofilm, anti-oxidant, wound healing, cytotoxic and antiviral activities. Journal of Trace Elements in Medicine and Biology. 2015; 32, 30-39.
6. Alam H, Khatoon N, Raza M, et al. Synthesis and characterization of nano selenium using plant biomolecules and their potential applications. BioNanoScience. 2019; 9(1), 96-104.
7. Hassanien R, Abed-Elmageed A, Husein Z. Eco-Friendly Approach to Synthesize Selenium Nanoparticles: Photocatalytic Degradation of Sunset Yellow Azo Dye and Anticancer Activity. ChemistrySelect. 2019; 4(31), 9018- 9026.
8. Prashant K, Suresh G, Trupti P, et al. Plant extract assisted eco-benevolent synthesis of selenium nanoparticles—A review on plant parts involved, Characterization and their recent applications, Journal of Chemical Reviews. 2020; 2(3), 157-168. doi:10.22034/jcr.2020.106601
9. Tripathi M, et al. Biosynthesis of highly stable fluorescent selenium nanoparticles and the evaluation of their photocatalytic degradation of dye. BioNanoScience. 2020; 1-8.
10. Tianyu L, Huaping X. Selenium-Containing Nanomaterials for Cancer Treatment. Cell Reports Physical Science. 2020; 100111, July 22.
11. Praveen S, Ravikanth N, Pawan G, et al. Improved extraction of intracellular biogenic selenium nanoparticles and their specificity for cancer chemoprevention. Journal of Nanomedicine & Nanotechnology. 2014; 5:2, 1000194.
12. Ali N, Sawsan M, Fatma S. Evaluation of selenium nanoparticles as a potential chemopreventive agent against lung carcinoma. International Journal of Pharmaceutical Biological and Chemical Sciences. 2013; 2(4), 38-46.
13. Sasidharan S, Sowmiya R, Balakrishnaraja R. Biosynthesis of selenium nanoparticles using citrus reticulata peel extract. World Journal of Pharmaceutical Research. 2015; 4(1), 1322-1330.
14. Sharma G. Biomolecule-mediated synthesis of selenium nanoparticles using dried Vitis vinifera (raisin) extract. Molecules. 2014; 19(3), 2761-2770.
15. Deepa B, Ganesan V. Bioinspiredsynthesis of selenium nanoparticles using flowers of Catharanthus roseus (L.) G. Don. and Peltophorum pterocarpum (DC.) Backer ex Heyne—a comparison. International Journal of ChemTech Research. 2015; 7(2), 725-733.
16. Jay V, Shafkat R. Green synthesis of selenium nanoparticles using Allium sativum extract. Asian Journal of Life sciences. 2017; 6(3), 436-440.
17. Anu K, Singaravelu G, Murugan K. Green-synthesis of selenium nanoparticles using garlic cloves (Allium sativum): biophysical characterization and cytotoxicity on vero cells. Journal of Cluster Science. 2017; 28(1), 551-563.
18. Vyas J, Rana S. Antioxidant activity and green synthesis of selenium nanoparticles using allium sativum extract. International Journal of Phytomedicine. 2017; 9, 634.
19. Thangavelu S, Periyakali Saravana B and Subramaniyam K. Green synthesis of selenium nanoparticles from sodium selenite using garlic extract and its enrichment on Artemia nauplii to feed the freshwater prawn Macrobrachium rosenbergii postlarvae. Research Journal of Chemistry and Environment. 2017; 21(10), 1-12.
20. Jay V and Shafkat R. Synthesis of seleniumnanoparticles using Allium sativum extract and analysis of their antimicrobial property against gram positive bacteria. The Pharma Innovation Journal. 2018; 7(9): 262-266.
21. Vyas J, Rana H. Antioxidant activity and biogenic synthesis of selenium nanoparticles using the leaf extract of aloe vera. International Journal of Current Pharmaceutical Research. 2017; 9, 147-152.
22. Kapur M, Soni K, Kohli K. Green synthesis of selenium nanoparticles from broccoli, characterization, application and toxicity. Advanced Techniques in Biology & Medicine. 2017; 5(1), 2379-1764.
23. Dongxiao C, Tingting L, Liquian S et al. Green synthesis of selenium nanoparticles with extract of hawthornfruit induced HepG2 cells apoptosis. Pharmaceutical biology. 2018; 56(1), 528-534.
24. Sivakumar C, Jeganathan K. In-vitro cytotoxicity of java tea mediated selenium nanoballs against L6 cell lines. Journal of Drug Delivery and Therapeutics. 2018; 8(6), 195-200.
25. Mellinas C., Jiménez A, Garrigós C. Microwave-Assisted Green Synthesis and Antioxidant Activity of Selenium Nanoparticles Using Theobroma cacao L. Bean Shell Extract. Molecules. 2019; 24(22), 4048.

26. Soumya M, Shrudhi S, Happy A, et al. Efficacy of Biogenic Selenium Nanoparticles from an extract of ginger towards evaluation on anti-microbial and antioxidant activities. Colloid and Interface Science Communications. 2019; 29, 1-8.
27. Dabei F, Li L, Zhizhen L, et al. Biosynthesis of selenium nanoparticles and their protective, antioxidative effects in streptozotocin induced diabetic rats. Science and Technology of Advanced Materials. 2020; 21(1), 505-514.
28. Nayeem M, Sachin O, Raghvendra B. Rapid and sizecontrolled biosynthesis of cytocompatible selenium nanoparticles by Azadirachta indica leaves extract for antibacterial activity. Materials Letters. 2020; 264, 127353.
29. Vetrivel C, Durairaj K, Kalaimurugan D. Green synthesis of selenium nanoparticles mediated from Ceropegia bulbosa Roxb extract and its cytotoxicity, antimicrobial, mosquitocidal and photocatalytic activities. Scientific Reports. 2021; 11:1032. doi: 10.1038/s41598-020-80327-9.
30. Ecem E, Aydın A. Selenium nanoparticles synthesized via green methods from Calluna vulgaris extract: Exploring their antioxidant and antibacterial activities. International Journal of Secondary Metabolite. 2024; 11(3), 462–471. doi: 10.21448/ijsm.1415795.
31. Georgia B, Sandra S, Genickson J, et al. Green synthesis of selenium nanoparticles mediated aqueous extract of Euphorbia Tirucalli and its antimicrobial and cytotoxic activities. African Journal of Biomedical Research. 2024; 27(3); 1035-1042. doi: 10.53555/AJBR.v27i3.2748.
32. Krystyna P. Plant extracts for production of functionalized selenium nanoparticles. Materials. 2024; 17, 3748. doi: 10.3390/ma17153748.
33. Hua C , Li W, Shuqing J, et al. Green synthesis of selenium nanoparticles by grape seed extract synergized with ascorbic acid: Preparation optimization, structural characterization, and functional activity. Foods. 2025; 14, 3002, 1-17. doi: 10.3390/foods14173002.
34. Le S , Man L, Yingxiu W, et al. Biosynthesis of selenium nanoparticles from Rosa rugosa extract: Mechanisms and applications for sustainable crop protection. Agronomy. 2025; 15, 2385. doi: 10.3390/agronomy15102385.
35. Mohamed E, Heba A, Gehan A, et al. Eco-friendly synthesis of Balanites aegyptiaca-derived selenium nanoparticles: extract and assessment of their anticancer, antimicrobial, cytogenetic and molecular docking insights. Scientific Reports. 2026; 16: 4721. doi: 10.1038/s41598-026-35358-z.
36. Sama H, Nada K, Esraa O, et al. Facile green synthesis of selenium nanoparticles using olive (Olea europaea) leaf extract and their antimicrobial and antibiofilm properties. Scientific Reports. 2026; 16:15224. doi: 10.1038/s41598-026-47329-5.
37. Halvin A, Subramani K. Broccoli-mediated green synthesis of selenium nanoparticles with potent antioxidant and antimicrobial activities: Experimental and molecular docking insights. Food Chemistry Advances. 2026; 10, 101260. doi: 10.1016/j.focha.2026.101260.
38. Aya E, Amr M and Heba A. Biosynthesis of selenium nanoparticles by Aloe vera leaf extract and its biomedical applications. Discover Nano. 2026; 21:91. doi: 10.1186/s11671-026-04489-7.
39. Anjali S and Sheetal S. Phytochemical analysis and free radical scavenging potential of herbal and medicinal plant extracts. Journal of Pharmacognosy and Phytochemistry. 2013; 2(4), 22–29.
40. Skehan P, Storeng R, Scudiero D, et al. New colorimetric cytotoxicity assay for anticancerdrug screening, Journal of National Cancer Institute. 1990, 82, pp.1107–1112.
41. Isaac G, Gabriela T, Daniel U, et al. Green synthesis of silver nanoparticles with phytosterols and betalain pigments as reducing agents present in cactus. Myrtillocactus geometrizans. 2020; 5, 3361–3369.
42. Su W, Yang H, Wang C. Biosynthesis and antioxidation of nano-selenium using lemon juice as a reducing agent. Green Processing and Synthesis. 2021; 10: 178–188.
43. Nahid S, Saba Z, Fatemesh K. Selenium nanoparticles synthesis, invitro cytotoxicity, antioxidant activity and interaction studies with ct-DNA and HAS, HHb and Cyt c serum proteins. Biotechnology Reports. 2021; 30, e00615.
44. Mustafa M. El-Z, Mostafa M. E, Hani A, et al. The antimicrobial, antioxidant, and anticancer activity of greenly synthesized selenium and zinc composite nanoparticles using Ephedra aphylla extract. Biomolecules. 2021; 11, 470, 1-17.
45. Naiyer S, Wajahatullah K. Phytosterols as a natural anticancer agent: Current status and future perspective, Biomedicine & Pharmacotherapy. 2017; 88, 786-794.
46. Shenbagamoorthy S, Ramar T, Vellingiri S, et al. γ-Sitosterol from Acacia nilotica L. induces G2/M cell cycle arrest and apoptosis through c-Myc suppression in MCF-7 and A549 cells. Journal of Ethnopharmacology. 2012; 141(3), 803-809.
47. Wen W, Shih C, Yueh L, et al. Stigmasterol inhibits cancer stem cell activity in endometrial cancer by repressing IGF1R/mTOR/AKT pathway, Journal of Functional Foods. 2022; 99,105338, 1-12.